<u>**Supplementary Material**</u>

Predictability of the Early Summer Surface Air Temperature over Western South Asia

Irfan Ur Rashid[1], Muhammad Adnan Abid[*2,6], Marisol Osman[3,4], Fred Kucharski[2,6], Moetasim Ashfaq[5], Mansour Almazroui[6,7], José Abraham Torres-Alavez[8], Muhammad Afzaal[1].

1. *Research and Development Division, Pakistan Meteorological Department, Islamabad, Pakistan*
2. *Earth System Physics, Abdus Salam International Centre for Theoretical Physics (ICTP), Trieste, Italy*
3. *Karlsruhe Institute of Technology, Karlsruhe, Germany*
4. *Universidad de Buenos Aires, Facultad de Ciencias Exactas y Naturales, Departamento de Ciencias de la Atmósfera y los Océanos, CONICET – Universidad de Buenos Aires, Centro de Investigaciones del Mar y la Atmósfera (CIMA), CNRS – IRD – CONICET – UBA, Instituto Franco-Argentino para el Estudio del Clima y sus Impactos (IRL 3351 IFAECI), Buenos Aires, Argentina.*
5. *Computational Sciences and Engineering Division, Oak Ridge National Laboratory, Oak Ridge, TN, USA.*
6. *Centre of Excellence for Climate Change Research (CECCR)/Department of Meteorology, King Abdulaziz University, Jeddah, Saudi Arabia.*
7. *Climatic Research Unit, School of Environmental Sciences, University of East Anglia, Norwich, UK*
8. *Institute for Atmospheric and Climate Science, ETH Zürich, Zürich, Switzerland*

Submitted to
Climate Dynamics

February 2023

Corresponding Author:

*M. Adnan Abid
Earth System Physics,
Abdus Salam International Centre for Theoretical Physics (ICTP),
Strada Costiera 11, I-34151, Trieste, Italy.
Email: mabid@ictp.it
ORCID: https://orcid.org/0000-0002-7389-7977

Supplementary Figure List

Figure S1: a-d) Mean Surface air temperature (SAT) for NCEP, MERRA-2, CRU and CPC during early summer season (May-June: MJ) respectively; **e-h)** same as of (a-d) but for the Standard deviation of the SAT; Units (°C).

Figure S2: a-c) ERA5 SAT anomaly composite maps for the warm years (referred as $SATI_p$; units (°C)), corresponding Z200 (units: m) and SST anomalies (units (°C)) for the period 1981-2022; **d-f)** same as (a-c) but for colder temperature composite anomalies (referred as $SATI_n$). Warm and Cold temperature years are selected based on ± 1°C standard deviation of the ERA5 SATI over WSA region (shown in Table 1).

Figure S3: Early summer season (May-June; MJ) Anomaly Correlation Skill of SAT based on **a)** NCEP (1981-2022), **b)** MERRA-2 (1981-2022), **c)** CRU (1981-2021) and **d)** CPC (1981-2022) over WSA region.

Figure S4: a-c) Signal, Noise and Signal-to-Noise (S/N) ratio for El Niño and **d-f)** La Niña years of SAT during early summer season for the period 1981-2022. Statistical significance is shown as stippling at 95% confidence level using F-test.

Supplementary Tables

Table S1: Detail of Observational and reanalysis datasets used in the study.

Table S2: The warm and cold phase of ENSO referred as El Niño and La Niña respectively, where El Niño/La Niña years are defined based on ± 0.5°C standard deviation of Niño3.4 SST index.

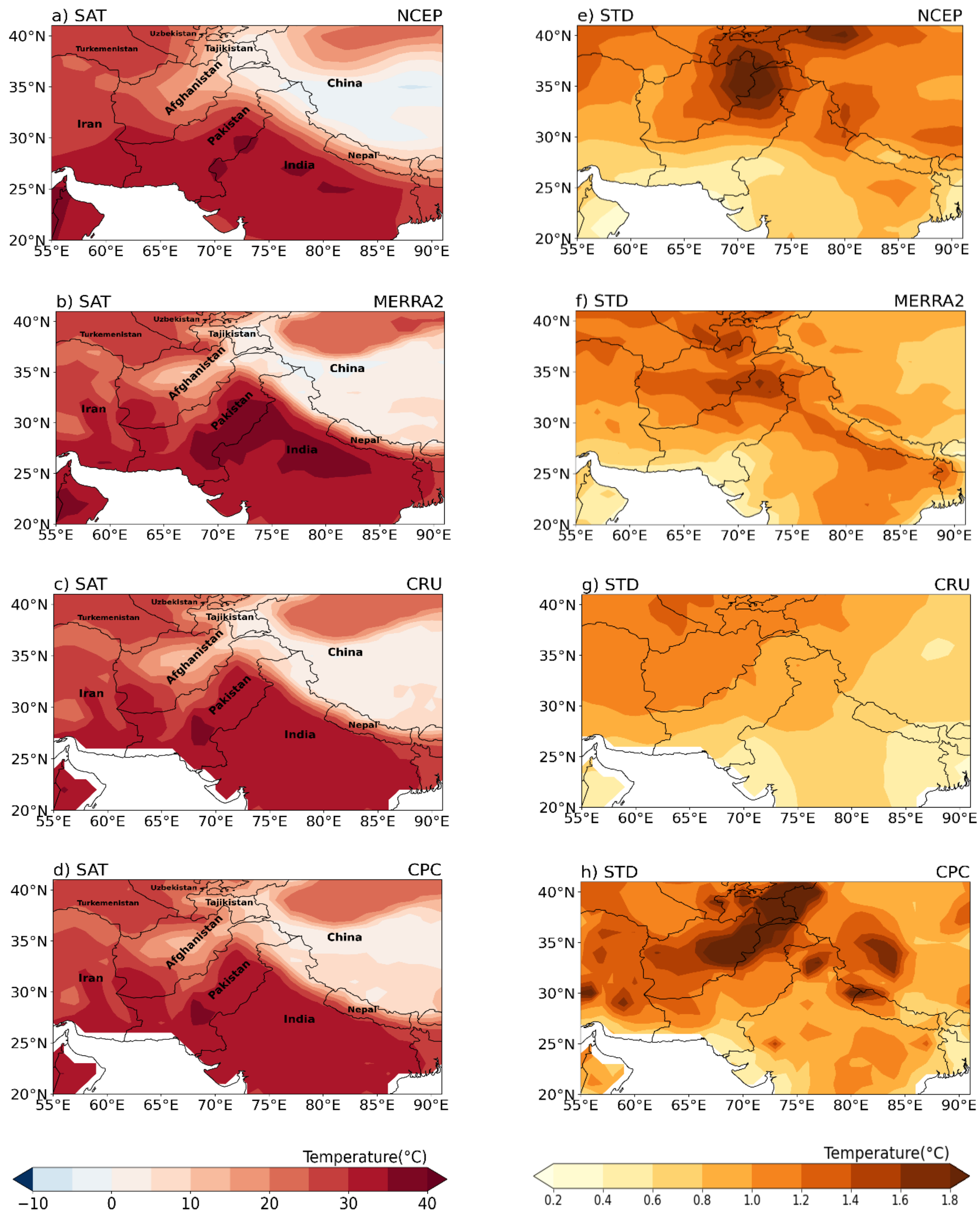

Figure S1: a-d) Mean Surface air temperature (SAT) for NCEP, MERRA-2, CRU and CPC during early summer season (May-June: MJ) respectively; **e-h)** same as of (a-d) but for the Standard deviation of the SAT; Units (°C).

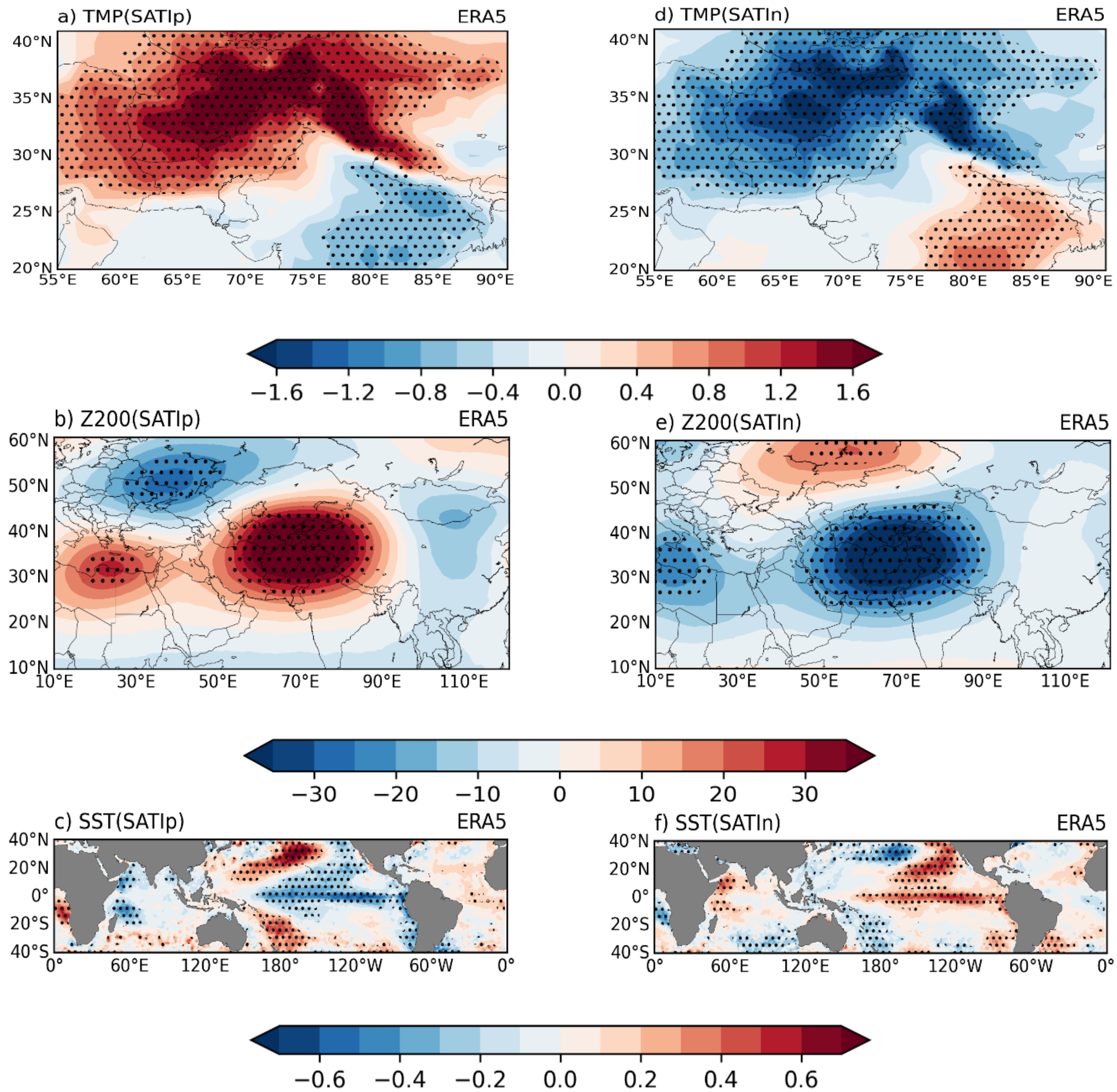

Figure S2: a-c) ERA5 SAT anomaly composite maps for the warm years (referred as $SATI_p$; units (°C)), corresponding Z200 (units: m) and SST anomalies (units (°C)) for the period 1981-2022; **d-f)** same as (a-c) but for colder temperature composite anomalies (referred as $SATI_n$). Warm and Cold temperature years are selected based on ± 1°C standard deviation of the ERA5 SATI over WSA region (shown in Table 1).

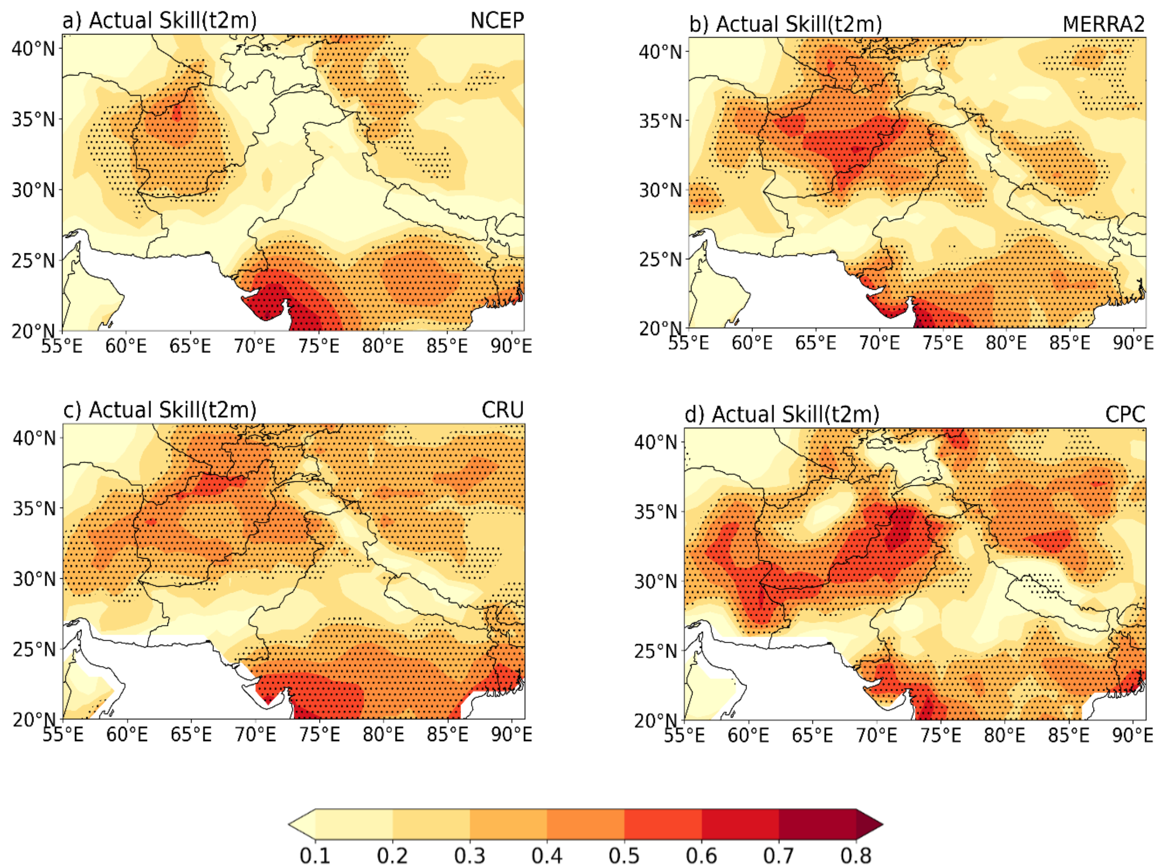

Figure S3: Early summer season (May-June; MJ) Anomaly Correlation Skill of SAT based on **a)** NCEP (1981-2022), **b)** MERRA-2 (1981-2022), **c)** CRU (1981-2021) and **d)** CPC (1981-2022) over WSA region.

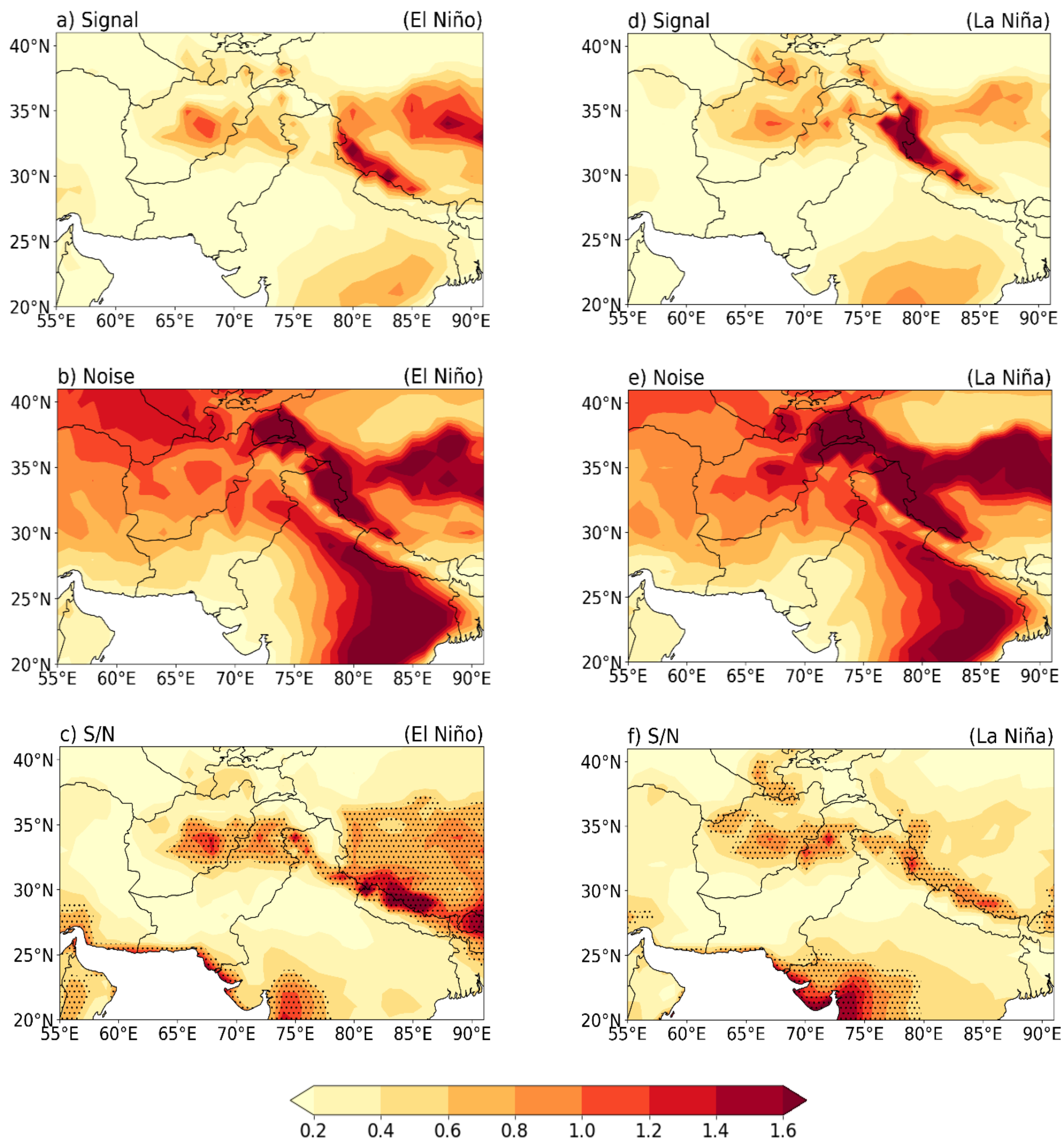

Figure S4: a-c) Signal, Noise and Signal-to-Noise (S/N) ratio for El Niño and **d-f)** La Niña years of SAT during early summer season for the period 1981-2022. Statistical significance is shown as stippling at 95% confidence level using F-test.

Table S1: Detail of Observational and reanalysis datasets used in the study.

Observational/ reanalysis datasets	Resolution (lat x lon)	Period	References	Data types
Fifth generation European Re-Analysis (ERA5)	0.25° x 0.25°	1981-2022	(Hersbach *et al.*, 2020)	reanalysis
National Centre for Environmental Prediction (NCEP)/National Centre for Atmospheric Research (NCAR)	2.5° x 2.5°	1981-2022	(Kalnay *et al.*, 1996)	reanalysis
Climate Research Unit (CRU v4.04)	0.5° x 0.5°	1981-2021	(Harris *et al.*, 2020)	observational
Modern-Era Retrospective Analysis for Research and Applications, Version 2 (MERRA-2)	0.5° x 0.625°	1981-2022	(Gelaro *et al.*, 2017)	reanalysis
Climate Prediction Center (CPC)	0.5° x 0.5°	0.5° x 0.5°	https://psl.noaa.gov/data/gridded/data.cpc.globaltemp.html	observational

Table S2: The warm and cold phase of ENSO referred as El Niño and La Niña respectively, where El Niño/La Niña years are defined based on ± 0.5°C standard deviation of Niño3.4 SST index.

ENSO phases	Years
El Niño (9)	1982, 1983, 1987, 1991, 1992, 1993, 1997, 2015, 2019
La Niña (10)	1981, 1984, 1985, 1988, 1989, 1996, 1999, 2000, 2008, 2022